

## Small Angle Neutron Scattering Study of Lysozyme–Sodium Dodecyl Sulfate Aggregates

Anna Stenstam,<sup>\*,†</sup> Gemma Montalvo,<sup>‡,§</sup> Isabelle Grillo,<sup>§</sup> and Michael Gradzielski<sup>||</sup>

Physical Chemistry I, Lund University, P.O. Box 124, SE-221 00 Lund, Sweden, Departamento Química Física, Universidad de Alcalá, Spain, Institute Laue-Langevin, BP 156, F-38042 Grenoble, France, and Lehrstuhl für Physikalische Chemie I, Universität Bayreuth, D-95440 Bayreuth, Germany

Received: May 9, 2003; In Final Form: July 24, 2003

The lysozyme–sodium dodecyl sulfate–water system features several interesting aggregation phenomena and is also of interest as it constitutes a model system for mixtures of a charged colloid with an oppositely charged surfactant, as both colloid and surfactant are pure and monodisperse compounds. The structure of such mixed protein–surfactant systems has been investigated by means of SANS contrast variation experiments. Two interesting issues of protein–surfactant aggregation are discussed. First, a new set of data on the structure of the protein–surfactant complex in solution is added to the discussion of whether the model of “beads on a necklace”, “protein decorated micelles”, or “flexible helix” is most appropriate. It is our conclusion that the compact globule of lysozyme does not fit well into any of the mentioned models. Instead, transient clusters of lysozyme–SDS aggregates are proposed for the  $L_1$  phase and more strongly bound locally linear clusters for the gel phase. Second, the structure and formation of a homogeneous, transparent gel at room temperature is analyzed and compared to the well-studied heat-set globular gels. The gel structure in different ionic strengths, lower than the one caused by naturally occurring buffer salts has also been analyzed and it seems that small amounts of salt render the system a more repulsive character than salt-free conditions. In addition to the equilibrated samples studied with the contrast variation technique, the complexation has been studied over time.

## Introduction

Protein–surfactant aggregation in oppositely charged systems is a fascinating phenomenon, among many things because of the delicate balance between the forces of interaction mainly stemming from electrostatic forces and hydrophobic interactions, the well-defined colloid, i.e., the monodisperse protein, the discord about the complex structure and the practical importance of the gels. In addition, gel formation is relatively slow—requiring several weeks to months—and the structural changes taking place are complex.

In this work, the oppositely charged system of lysozyme and sodium dodecyl sulfate (SDS) in water is studied. Lysozyme is a small, globular enzyme with a slightly ellipsoidal shape. The main chain fold in solution is very close to that of the crystal,<sup>1</sup> revealed for the first time by Blake et al. 1965.<sup>2</sup> The lengths of the ellipsoidal axes are 15 and 22 Å, respectively.<sup>3</sup> The isoelectric point is at pH 11 and in a neutral aqueous solution lysozyme has 18 cationic and 10 anionic sites, i.e., a net charge of +8.<sup>4</sup> At low ionic strength the protein is predominantly monomeric but dimer- and oligomerization occurs in concentrated solutions.<sup>5</sup> Four disulfide bridges stabilize the globular shape of the protein so that an unfolding does not necessarily follow on denaturation.<sup>6</sup> The anionic surfactant SDS has a critical micellization concentration (cmc) of 8 mM and associates strongly to the protein due to electrostatic as well as hydrophobic attraction.<sup>7,8</sup>

The phase behavior for the lysozyme–SDS–water system in the range of 80–100 wt % water has been fully described by Morén et al. and is here reviewed.<sup>9</sup> Three different phases are obtained within these concentration limits. First, a precipitate of the net-neutralized macromolecule is formed,  $Ly(DS)_8$ .<sup>10,11</sup> With increasing surfactant concentration a critical association concentration,  $cac$ , is reached and surfactant molecules associate on the protein–surfactant salt. This leads to complexes with a net-negative charge. At concentrations just above the  $cac$  the repulsion caused by the negative charge is not yet large and the hydrophobic attraction between the complexes balance well for a gel to be formed.<sup>10</sup> At higher concentrations the system is dominated by repulsion and soluble protein–surfactant complexes form a clear nonviscous solution phase,  $L_1$ .

The structure of soluble protein–surfactant complexes has been studied and debated for more than 20 years.<sup>12–15</sup> Different models have been proposed from which some agreement seems to surface, that the surfactant is micelle-like and associated as a spherical aggregate to the protein.<sup>16–18</sup> The protein molecule is in these models regarded as relatively flexible and composed of blocks of hydrophilic or hydrophobic character. As such they are “decorating” the micelles or being decorated by micelles distributed along the polypeptide chain.<sup>14,17</sup> However, lysozyme cannot readily be considered as a flexible polymer due mainly to the disulfide bridges. As a result heat-denatured lysozyme is only slightly larger ( $R_H = 22$  Å)<sup>19</sup> than the native globule ( $R \approx 18$  Å)<sup>15,19,20</sup> and complexes between SDS and lysozyme under dilute conditions (55–100 S/P) have been found to be only slightly larger ( $R_H = 32$ ), i.e., presumably one still has a compact globular lysozyme.<sup>15</sup> Hence, the question of how these complexes are structured is not easily resolved and one intention of this paper is to contribute to the solution.

\* To whom correspondence should be addressed. Please use postal address, e-mail (anna.stenstam@fkem1.lu.se), or fax (+46-46-222 44 13).

<sup>†</sup> Lund University.

<sup>‡</sup> Universidad de Alcalá.

<sup>§</sup> Institute Laue-Langevin.

<sup>||</sup> Universität Bayreuth.

The second focus of the present work is the formation and structure of the protein–surfactant gel. Pure lysozyme gels can be formed by heat denaturation. The resulting gels may be either turbid, due to random aggregation, or transparent due to a more homogeneous aggregation.<sup>21,22</sup> The manner of aggregation seems to be controlled by the electrostatic interaction, i.e., by the pH and ionic strength. In this work we form transparent and elastic gels with a minimum of electrolyte present as well as with low concentrations of added  $\text{NaCl}_{\text{aq}}$ . The maximal electrostatic interaction is obtained when the truly ternary system is used, i.e., when the stoichiometric salt  $\text{Ly}(\text{DS})_8$  is used as the protein source instead of lysozyme because the latter is crystallized with buffer salts. It is possible that the protein–surfactant gels can reproduce the behavior and formation mechanisms of the linear aggregation pattern of the heat-set gels.<sup>23</sup> If this is the case the question is whether the building blocks are related in composition to the soluble protein–surfactant complexes. Moreover, if the aggregation is linear the possibility to extend an understanding of this system to the protein fibril formation causing malfunctions such as Alzheimer's disease is a worthy challenge.

To fully understand the structures of the different phases, a small angle neutron scattering (SANS) study with the contrast variation method applying mainly three different contrasts has been used. In addition, four samples have been measured at different times over a period of four months.

Finally, the use in this work of both the ternary system,  $\text{Ly}(\text{DS})_8$ –SDS–water, and the pseudoternary system, lysozyme–SDS–water, as well as intermediate versions,  $\text{Ly}(\text{DS})_8$ –SDS– $\text{NaCl}_{\text{aq}}$ , i.e., samples with a systematic variation of the ionic strength, renders it possible to generalize the thermodynamic discussion based on molecular mechanisms. It should be noted that our system constitutes a model system for a mixture of a charged colloid with an oppositely charged surfactant, as the colloid in this case is a well-characterized monodisperse compound.

## Experimental Section

**(a) Materials.** Lysozyme (95%) from chicken egg white three times recrystallized, dialyzed, and lyophilized was obtained from Sigma. Sodium dodecyl sulfate, SDS, was supplied by BDH. Perdeuterated SDS was synthesized by Cambridge Isotope Laboratories Inc., and NaCl obtained from Riedel-de Haën. Millipore filtered  $\text{H}_2\text{O}$  and/or  $\text{D}_2\text{O}$  supplied by Dr. Glaser were used as solvent. Both protein and surfactant were used as received in the majority of the sample preparations, i.e., for samples in the pseudoternary system lysozyme–SDS–water. For the true ternary system the complex salt of lysozyme and dodecyl sulfate  $\text{Ly}(\text{DS})_8$  was used as the protein source. The complex salt,  $\text{Ly}(\text{DS})_8$ , was synthesized as described in a previous paper.<sup>10</sup> For some samples of the contrast variation the complex salt was prepared from lysozyme and perdeuterated dodecyl sulfate,  $\text{Ly}(\text{DS})_{8(\text{d})}$ .

**(b) Phase Determination.** In the concentration regime of 80–100 wt % water the phase behavior of the lysozyme–SDS as well as the  $\text{Ly}(\text{DS})_8$ –SDS system features three different phases:<sup>9,10</sup> first, at small SDS content a solid precipitate of the complex salt  $\text{Ly}(\text{DS})_8$  appears, (S); second, a transparent gel with slightly bluish color (G); third, a soluble protein–surfactant complex that presents itself as an isotropic, clear, nonviscous solution phase ( $\text{L}_1$ ). SANS experiments have been performed on  $\text{L}_1$ , G, and also on the two-phase equilibrium between the gel and isotropic solution. The identification of the bluish solutions as two-phase samples and their subsequent characterization can be found in our preceding work.<sup>10,24</sup>

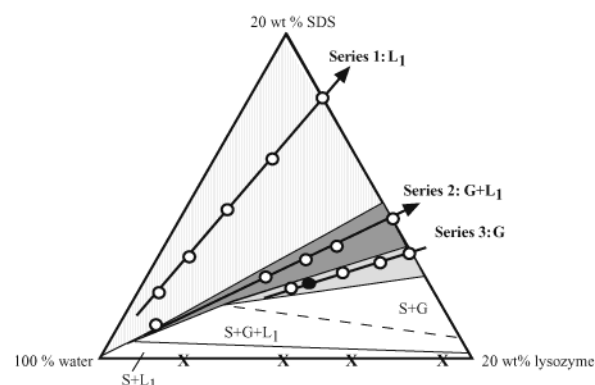


**Figure 1.** Schematic phase diagram redrawn from Morén et al.<sup>9</sup> The lines indicate the three series studied with the contrast variation method, and the points, the different compositions: ●, the gel composition studied in different ionic strengths. In addition, the concentrations of lysozyme in the four samples measured in the binary system is shown, ×.

In Figure 1 the three studied dilution lines are indicated with marks showing the composition of the samples studied by contrast variation and the sample studied in different ionic strengths. The samples analyzed by the contrast variation technique were prepared to have identical molar compositions. The detailed composition of the samples is available as Supporting Information. The samples were prepared one month before being measured by SANS except for the time-evolution study where the samples were prepared on the day of the first measurement. A few samples prepared to match each other in different contrasts had at the time of the measurement not the same physical appearance. This might be due to the differences between heavy and normal water, which can be of a complex nature, not in the scope of this paper.<sup>25</sup> These samples have not been analyzed in line with the contrast variation but are considered as representatives for their contrast and appearance at the time of measurement.

**(c) SANS—Experimental Details.** Measurements were performed on the instruments D22 and D11 at the Institute Laue-Langevin (ILL), Grenoble, France. The spectra were recorded for each sample at two or three different sample-to-detector distances, respectively. Thereby a range of the magnitude of the wave vector  $q$  from 0.003 to 0.4  $\text{\AA}^{-1}$  was covered. The neutron wavelength was fixed at 8 or 6  $\text{\AA}$ , respectively. The data were corrected for transmission and sample thickness and put on an absolute scale by a comparison with water scattering. Corrections and normalization were done by means of standard routines supplied by the ILL.<sup>26</sup> Three different contrast conditions were employed in series 1, 2, and 3:

(I) Samples with deuterated SDS (D-SDS) in  $\text{D}_2\text{O}$ : mainly lysozyme is seen (lysozyme contrast).

(II) Samples with deuterated SDS (D-SDS) in  $\text{H}_2\text{O}$ : mainly SDS and to a lesser extent lysozyme is seen (surfactant and lysozyme contrast).

(III) Samples with protiated SDS (H-SDS) in  $\text{D}_2\text{O}$ : mainly SDS and to a lesser extent lysozyme is seen (surfactant and lysozyme contrast).

In addition, for the study over time:

(IV) Samples where both protein and surfactant are protiated and dissolved in  $\text{H}_2\text{O}$ : a low contrast where mostly lysozyme is seen.

**(d) SANS—Theoretical Models.** The scattering curves are described by various models that shall be detailed in the following. In general the angular dependence of the scattering intensity,  $I(q)$ , of a system composed of interacting particles

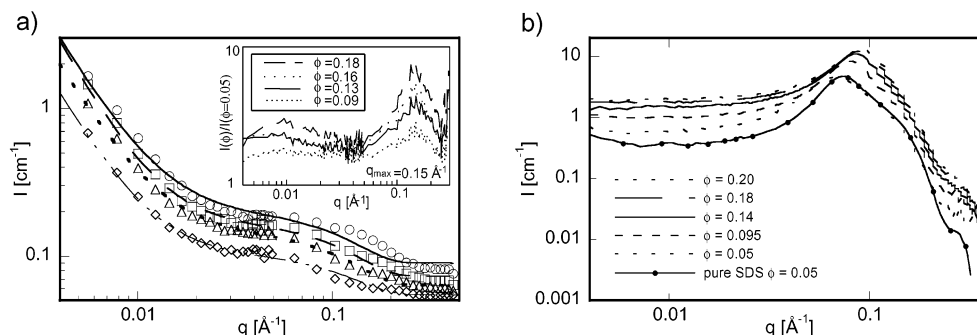


**Figure 2.** Series (Figure 1, series 1). (a) Scattering giving the lysozyme contrast (I), D-SDS in D<sub>2</sub>O. Fitted curves are given as lines, and 30% of the experimental data points are given as symbols. Key: full line and circles,  $\phi = 0.18$ ; dashed line and squares,  $\phi = 0.16$ ; dotted line and triangles,  $\phi = 0.09$ ; dashed-dotted line and diamonds,  $\phi = 0.05$ . See text for details on the fitting procedure. Inset: The scattering of lysozyme is here normalized by division to the scattering of the most dilute sample in the series ( $\phi = 0.05$ ) as well as to the volume fraction of lysozyme. (b) The scattering dominated by SDS for all samples within the series but lysozyme is not completely matched. The contrast (II) is given by D-SDS in H<sub>2</sub>O.

can be described as

$$I(q) = NP(q) S(q) \quad \text{with} \quad q = \frac{4\pi}{\lambda} \sin(\theta/2) \quad (1)$$

where  $N$  is the number density and  $P(q)$  the form factor of the particles and the structure factor  $S(q)$  describes the interaction between the particles.

The structure factor due to a cluster of particles can be described by means of a fractal model. By using an exponential cutoff with characteristic length  $\xi$ , Chen and Teixeira derived the corresponding fractal structure factor:<sup>27,28</sup>

$$S(q) = 1 + \frac{1}{(qR)^D} \frac{D\Gamma(D-1)}{(1 + (q\xi)^{-2})^{(D-1)/2}} \sin((D-1) \arctan(q\xi)) \quad (2)$$

where  $D$  is the fractal dimension,  $R$  is the radius of the fractal forming particles, and  $\Gamma$  is the gamma function.

For our case we consider a clustering of lysozyme molecules that have been shown before to be described well by rotational ellipsoids.<sup>29</sup> The form factor for randomly oriented rotational ellipsoids is given by<sup>30</sup>

$$P(q) = P(0) \int_0^{\pi/2} P(q, \beta) \cos \beta d\beta \quad (3)$$

where  $\beta$  is the angle between  $q$  and the rotational axis.  $P(q, \beta)$  and  $P(0)$  are given by

$$\frac{P(q, \beta)}{P(0)} = [f(qa\sqrt{\cos^2 \beta + t^2 \sin^2 \beta})]^2 \quad (4)$$

where

$$f(x) = \frac{3(\sin x - x \cos x)}{x^3} \quad (5)$$

$$P(0) = \left[ \frac{4\pi}{3} ta^3 (\rho_p - \rho_0) \right]^2 \quad (6)$$

$ta$  is the length of the rotational half axis,  $a$  is the other half axis, and  $t$  is the ratio between the two axis.  $\rho_p$  and  $\rho_0$  are the scattering length densities of particle and solvent, respectively.

The interaction between charged micelles was taken into account by means of a random phase approximation for the structure factor  $S(q)$ ,<sup>31</sup> and the form factor of the micelles was modeled by the ellipsoidal model given above.

For the scattering length densities of D<sub>2</sub>O and H<sub>2</sub>O we employed  $63.6 \times 10^9$  and  $-5.6 \times 10^9$  cm<sup>-2</sup>, respectively. For

protiated and deuterated dodecyl sulfate (DS) we used  $3.1 \times 10^9$  and  $68.0 \times 10^9$  cm<sup>-2</sup>, respectively. Finally for the pure lysozyme molecule we used  $20.0 \times 10^9$  cm<sup>-2</sup> (in pure H<sub>2</sub>O) and  $37.0 \times 10^9$  cm<sup>-2</sup> (in pure D<sub>2</sub>O).

## Results and Discussion

**1. Soluble Protein–Surfactant Complex (L<sub>1</sub>).** The scattering data for this series (Figure 1, series 1) are presented in Figure 2. Figure 2a shows the lysozyme contrast, and Figure 2b, the SDS contrast. It was realized that the scattering from the surfactant dominates even when lysozyme contributes to the intensity, i.e., contrast II and III are almost identical. Therefore only contrast II is presented, in Figure 2b.

The lysozyme contrast data in Figure 2a for  $q > 0.03$  Å<sup>-1</sup> can be described with a model of rotational ellipsoids where the shape of the lysozyme molecule is fixed to the one known from the crystal structure, i.e., minor axis  $a = 15$  Å and major axis  $ta = 22.5$  Å.<sup>2</sup> Further, the lysozyme contrast does not reveal a peak such as the one seen for SDS (Figure 2b), nor does the intensity at low  $q$  values decrease or level off. Instead, there is an increase in intensity for low  $q$  values.

The absence of a correlation peak in Figure 2a can, if lysozyme nonetheless is solubilized in micelles, only mean that the number of pure surfactant micelles is much larger than the ones associated with a protein molecule. Thus, a large proportion of the surfactant is not contained in the same aggregates as the protein. The pronounced increase for low  $q$  values indicates an effectively attractive pair-potential between the protein molecules and such an attractive short-range pair potential between the protein–surfactant complexes is expected. In two recent papers we have argued that it is valid throughout the phase diagram, where it is balanced by repulsive (electrostatic) interactions.<sup>10,24</sup> The repulsive component is the reason these samples do not phase separate despite the attraction. In fact, samples prepared within the L<sub>1</sub> area have shown a macroscopic stability and remained visually the same over several years. The increase in lysozyme scattering for low  $q$  values follows a scaling law with  $q^{-D}$  with  $D = 2.1$ – $2.4$ . Such an increase could, if only the SANS data were considered, be explained either by a fractal aggregation or by allowing for a dual state of lysozyme and subsequently two different protein–surfactant complexes where one would correspond to large aggregates. Valstar et al. have argued in favor of the latter on the basis of dynamic and static light scattering experiments.<sup>15</sup> However, the larger complex in their discussion only consists of one or two protein molecules and thus cannot account for the magnitude of the



increase reported here, whereas for an interpretation of the intensity in the low  $q$  range by large aggregates of unfolded proteins at least 20–50 lysozyme molecules would have to be aggregated. Furthermore, due to the observed slope of  $-2$ , they would have to be arranged in a sheetlike structure. This is not only very unlikely due to the characteristics of lysozyme,<sup>6,32–34</sup> it is also not supported by thermodynamical calculations,<sup>10</sup> diffusion NMR,<sup>24</sup> imaging by cryo-transmission electron microscopy,<sup>35</sup> or simply the nonviscous<sup>36</sup> transparent appearance of the samples.

Consequently, we applied a model of fractal aggregation in which the SANS intensity is calculated according to eq 1 and in which we used a form factor of prolate ellipsoids, eq 3, where we fixed the axis to  $a = 15$  Å and  $ta = 22.5$  Å, and the fractal structure factor given by eq 2. It should be noted that to obtain good fits, it is not possible to fix the radius  $R$  of the fractal subunits equal to the size of the lysozyme molecules but it has to be used as a free fit parameter. With this model a good agreement to the experimental data in the low  $q$  range is observed, Figure 2a. We find that the fractal dimension  $D$  remains relatively constant between 2.2 and 2.3; i.e., the fractal packing is relatively dense. The radius  $R$  of the fractal subunits, which determines where the increase in  $q$  starts, is nearly constant at 82–87 Å; i.e., the subunits are significantly larger than an individual lysozyme molecule. Accordingly, one would speculate that these subunits are composed of several lysozyme molecules that are grouped densely together. No cluster size  $\xi$  is given, as in the scattering curves one sees a continuous increase in the intensity toward low  $q$ , which means that one is not yet in a  $q$  range to see this length. Accordingly, its value obtained from the fit procedure is just a very large number, which has to be significantly larger than  $2\pi/q_{\min} = 2000$  Å.

Thus our structural model based on the SANS results would be that on a local level lysozyme molecules are grouped densely together and form complexes. On a larger length scale these complexes form clusters. The relatively high values for  $D$  are expected for reaction-limited cluster aggregation (RLCA) and this is in agreement with the situation in lysozyme where one would not expect to have permanent formation of this fractal structure but instead a highly dynamic situation because the binding energies in the cluster formation are relatively weak dipole forces and/or hydrophobic contacts between the different lysozyme molecules which will allow for easy reversible binding/unbinding.

Focusing on the SDS contrast (Figure 2b), the measurements reveal a peak in the range  $0.07$ – $0.09$  Å<sup>-1</sup>, which corresponds to an interparticle spacing of 70–90 Å. The peak position depends on the total volume fraction,  $\phi$ , moving to higher  $q$  with increasing concentration. It should be noted that the scattering curves of the mixed SDS/lysozyme system are very similar to those of pure SDS solutions of the same concentration, as can be seen in the figure where, for comparison, the scattering curve for a SDS solution of 0.05 volume fraction is shown. This means that in the SDS/lysozyme system the large majority of the SDS is present in the same type of micelle as in the binary system. In comparison to the relation between  $q_{\max}$  and  $\phi$  that is displayed by pure protein solutions, the swelling is smaller, the exponent being 0.21 rather than 0.28 obtained by Renard et al.<sup>37</sup> The value of the exponent is given by three factors, geometry, interactions, and change of structure, e.g., growth. Thus, one explanation to the lower exponent is the effect of concentration-induced growth of the micelles.<sup>38</sup> However, it is not to be taken a priori that the SDS micelles behave as in the binary system because it has been shown that SDS micelles do

not grow with increasing ionic strength in the presence of a polymer.<sup>39</sup> Neither do rheological measurements on the system indicate a micellar growth.<sup>36</sup> Another explanation is that the aggregate–aggregate interaction is less repulsive, i.e., more attractive. This is possible as the peak in the SDS contrast is an effect of the correlations between SDS molecules of which one fraction is bound in protein–surfactant complexes and another fraction is found in pure surfactant micelles. The interaction between the micelles is repulsive but between the protein–surfactant complexes an attraction is expected, as discussed above. This attraction contributes to the overall scattering intensity profile and renders the total system less repulsive but still swelling.

A common next step in analyzing scattering spectra is to extract the structure function by dividing with a known (or skillfully guessed) form function. Here, the form function is not known due to lack in details of how associated surfactant molecules affect the form factor of lysozyme. We have nevertheless made an attempt to deduce more information from the measurements by dividing the spectra of the more concentrated samples by the most dilute within a series. Thereby at least more of the relative changes of the structure function are revealed. Thus, the data handling consists of three steps. First, a constant background was subtracted (a value obtained by Porod extrapolation). Second the spectra were normalized according to the volume fraction of the scattering species. Finally the spectra were divided by the most dilute curve within the series. This normalization procedure has been carried out for both the lysozyme (contrast I) and the SDS contrasts (II and III). It reveals a second peak with a peak position that is independent of concentration and consequently represents something other than the second-order Bragg peak of the one at 0.1. The peak position is at  $0.23$  Å<sup>-1</sup> (27 Å) when the scattering is from both surfactant and lysozyme, or mainly the surfactant is detected when the peak is observed at  $0.15$  Å<sup>-1</sup> (42 Å) when lysozyme is the main contributor to the intensity, as shown in the inset in Figure 2a. The indication of a neighbor-to-neighbor distance of the order of a lysozyme molecule can be interpreted as an oligomerization of proteins, i.e., protein molecules in a structure where they touch each other. The peak becomes pronounced with increasing concentration, as expected for a continued aggregation during which an increasing lysozyme–lysozyme correlation takes place.

**2. Two-Phase Bluish Solutions (G + L<sub>1</sub>).** A dilution series through the two-phase region where gel and soluble protein–surfactant complexes are in equilibrium, and into the pure L<sub>1</sub> phase at high dilution has been studied for contrast III (Figure 1, series 2). The results are presented in Figure 3a. First, it is important to note that the blue solutions scatter at much higher intensities compared to the samples in the L<sub>1</sub> region (one L<sub>1</sub> sample is included in the figure). Second, there is a large structural difference between the one-phase micellar sample and the two-phase, bluish solutions. The former exhibits a correlation peak that is characteristic for SDS micelles and in addition a relatively small increase at low  $q$  values. The latter spectra superimpose over a broad  $q$  range of  $0.01$ – $0.3$  Å<sup>-1</sup>. Aside from the lysozyme and SDS micellar form function at large  $q$  (note that both are of ellipsoidal shape with axis of 15–20 and 20–25 Å, and therefore are difficult to distinguish), the intensity increases with no specific correlation peak toward lower  $q$ . The absence of a micellar correlation peak shall not be taken as an absence of micelles. Instead, the presence of a larger aggregated structure, as indicated by the high intensity at lower  $q$ , dominates the scattering curve. The presence of micelles follows from

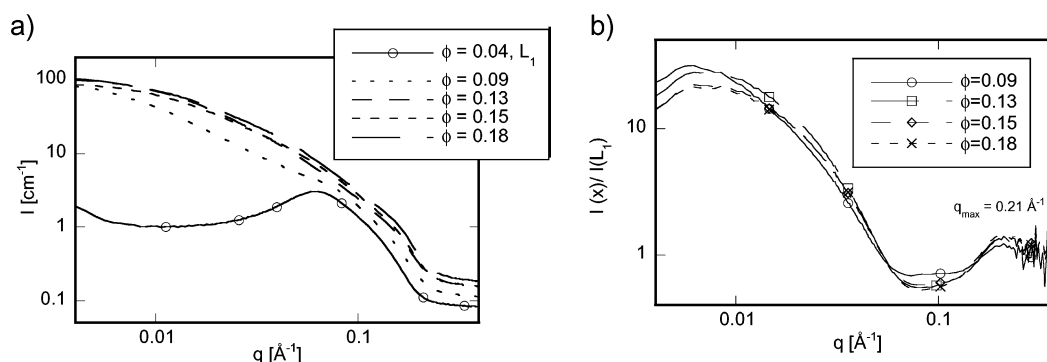


**Figure 3.** (a) Absolute intensities for four bluish solutions and one  $L_1$  sample in the same series (Figure 1, series 2). The contrast (III) is given by H–SDS in  $D_2O$ ; thus both protein and surfactant contribute to the intensity. The symbols are only added as guides for the legend. (b) Same bluish solution as in Figure 3a, compared to the  $L_1$  sample by normalization. The symbols are only added as a guide to the legend.

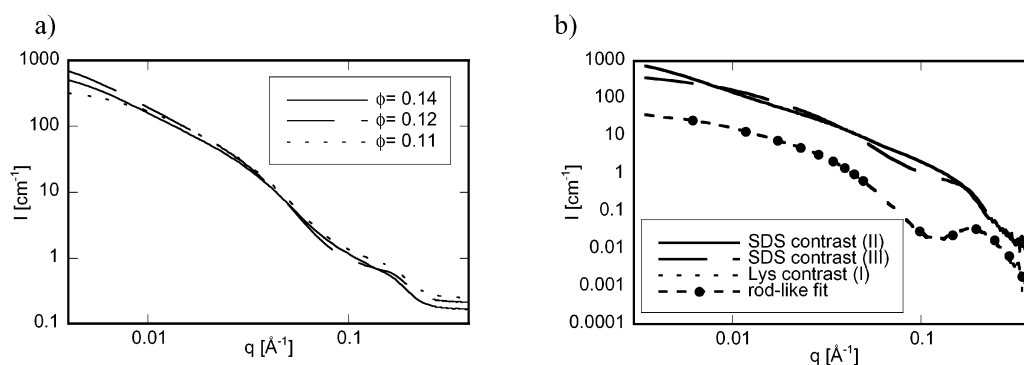


**Figure 4.** (a) Three gel samples along the swelling line (Figure 1, series 3), where the contrast is dominated by SDS, i.e., contrast III. (b) Gel sample at  $\phi = 0.12$  measured in three different contrasts and the fit to the lysozyme contrast.

Gibbs phase rules and the fact that the bluish solutions are two-phase equilibrium samples.<sup>24</sup>

A normalization of the spectra to the most dilute in the series, a  $L_1$  sample, shows a longer range of similarity for the bluish solutions, closer in composition to the micellar phase, Figure 3b. This is expected if we accept the idea of the two-phase sample being a dispersion of gel aggregates in a micellar  $L_1$  solution. Tie lines have not been reported for this two-phase area, but the orientation of the three-phase triangle within the diagram indicates that the more dilute bluish solutions have a larger fraction of  $L_1$  compared to the more concentrated, and hence also larger similarities to the  $L_1$  phase. The similarity is displayed as a horizontal,  $q$ -independent line in the normalized spectra. The more concentrated the bluish solutions are, the more this plateau turns into a minima at ca.  $0.09 \text{ \AA}^{-1}$ , thus indicating that the more concentrated samples are more structured. A third feature is found in Figure 3b. All bluish solutions exhibit a correlation peak at  $q = 0.21 \text{ \AA}^{-1}$  after normalization, which corresponds to a typical spacing of  $30 \text{ \AA}$ . This peak is similar to the one already seen for the samples in the  $L_1$  phase ( $q = 0.15 \text{ \AA}^{-1}$ , Figure 2a, inset) and is a sign of an oligomerization of lysozyme molecules. The increased pronouncedness of the peak with increasing concentration can be understood as an increasing number of neighbor-to-neighbor distances in the bluish solutions, as compared to the  $L_1$  sample. This should be due to larger aggregates with more correlated lysozyme–SDS complexes that explain the high intensity at low  $q$  values and the scattering of blue light. Thus, the aggregates must be larger than dimers or trimers. However, the correlation distance of  $30 \text{ \AA}$  does not rule out the possibility of a linear aggregate wider than one lysozyme molecule because the method is not sensitive enough for such details. Thus, the dimer model by Doi, applied by them to heat-set protein gels might be useful also for this

surfactant induced gelation. In their model dimers of globules, e.g., protein–surfactant complexes, are aggregated into multiples of two and form a wormlike cylinder.<sup>21,22</sup>

**3. Gel (G).** In Figure 4 it is shown that for the gel samples in the dilution series (Figure 1, series 3) all scattering curves within a specific contrast look relatively similar to each other but much different from the curves of the  $L_1$  phase (Figure 2).

The whole spectra with lysozyme contrast (one example shown in Figure 4b) could be fitted to a prolate ellipsoidal or rodlike model where the dimensions are much larger than for individual lysozyme molecules, because a pronounced increase in intensity occurs at low  $q$ . It indicates that in the gel a one-dimensional growth has taken place; i.e., one observes a structure of much lower fractal dimension than in the  $L_1$  phase. The radius of the local rodlike structure is relatively well-defined and is in the range  $45\text{--}55 \text{ \AA}$ , as can be inferred from the pronounced correlation peak. This range corresponds well to the dimer model mentioned for the bluish solutions and results in proposed structural subunits of 8 densely packed lysozyme molecules and the corresponding number of surfactant molecules.<sup>22</sup> This distance correlates well with the repeat distance of ca.  $45 \text{ \AA}$  obtained from a Fourier transformation of gel-images obtained by transmission electron microscopy. On the other hand the larger dimension of the aggregates is less precisely deduced from the fits because for linear objects the length becomes difficult to deduce accurately for sizes larger than the inverse of the smallest  $q$ . A schematic drawing of the structure proposed on the basis of the obtained results is presented in Figure 5.

Two samples were measured with the surfactant-dominated contrast II and the result from one is shown in Figure 4b together with the complementary contrasts, I and III. Contrast II shows only a continuous increase in intensity throughout the whole range, from  $q = 0.22$  to  $q = 0.003 \text{ \AA}^{-1}$ . Thus, no free surfactant

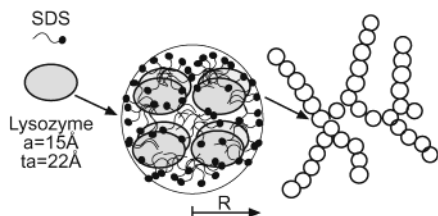


**Figure 5.** Proposed gel structure with a basic structural unit of radius  $R = 45\text{--}55\text{ \AA}$  that contains 8 lysozyme molecules. These form rigid and one-dimensional, i.e., rodlike, aggregates.

micelles seem to be present in the gel. This is supported by the NMR relaxation measurements presented by Morén et al. where the fast relaxation of SDS in the gel excludes the possibility of free spherical micelles.<sup>40</sup> The third contrast in Figure 4b (III) should also mainly give a surfactant contrast; however, the shape of the curve is different with a kink around  $0.16\text{ \AA}^{-1}$ .

**4. Salt Dependence of Gelation and Gel Structure.** It has been shown for the particular system under study that the gel formed in a saline solution is less elastic and more turbid.<sup>9</sup> It is understood that a more screened electrostatic interaction leads to a more disordered aggregation and hence a less transparent, less elastic gel.<sup>22</sup> Already the two systems lysozyme–SDS–water (pseudo-ternary) and  $\text{Ly}(\text{DS})_8$ –SDS–water (ternary) show this difference in a very pronounced way.<sup>36</sup> The gels presented so far have all been prepared with the lysozyme as received, i.e., with 5 wt % buffer salts. Now, instead 0–50 mM NaCl has been added to SDS solutions of  $\text{Ly}(\text{DS})_8$ . This range in ionic strength can only be achieved by using the complex salt  $\text{Ly}(\text{DS})_8$ , and this is the first time protein aggregation has been studied in the absence of buffer salts.

In Figure 6a are given scattering curves for samples in the gel phase that were prepared with a minimum amount of ionic strength present and that differ only with respect to the total concentration, contrast III. For these samples one observes a correlation peak in the range  $0.06\text{--}0.08\text{ \AA}^{-1}$  (corresponding to a repeat distance of  $75\text{--}100\text{ \AA}$ ), which moves to larger  $q$  with increasing concentration. Evidently there must be some ordering within the gel structure that corresponds to that distance. It could be due to a correlation between the rodlike structures observed within the gel phase but it fits also well to the next neighbor distance of the subunits in Figure 5.

Figure 6b shows that for all salt concentrations the scattered intensities superimpose at  $q$  values higher than  $0.08\text{ \AA}^{-1}$ ; i.e., the elementary structural unit in the gel aggregates is unaffected by the ionic strength. For the sample with no extra salt added the intensity profile shows a plateau until  $q = 0.02$ , after which it increases again, indicating the presence of large structures or effective attractive interactions between the lysozyme molecules.

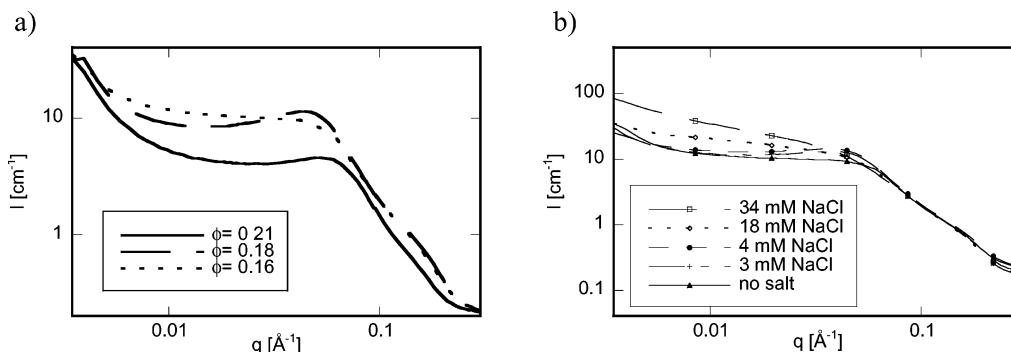


**Figure 6.** (a) Scattering for three gels prepared from the complex salt  $\text{Ly}(\text{DS})_8$  and SDS in  $\text{D}_2\text{O}$  (contrast III), thus at the lowest possible ionic strength. The three gels differ only by their water content. (b) Absolute intensities for the gel ( $\phi = 0.15$ ) prepared with different ionic strengths. Both surfactant and protein contribute to the intensity, i.e., contrast III. The symbols are only added as a guide for the legend.

For the samples with 18 mM or more of added NaCl (as well as the pseudo-ternary lysozyme–SDS gel in Figure 4a), the intensity increases all the way from  $0.2$  to  $0.005\text{ \AA}^{-1}$  with a kink at the point of  $0.06\text{ \AA}^{-1}$  and a subsequent change in slope. This behavior is similar to that observed for other systems such as lamellar liquid crystals with increasing ionic strength.<sup>41</sup> Thus, even in gelled samples the intermolecular distances ( $75\text{--}100\text{ \AA}$ ) remain unchanged but the correlation is lost with addition of salt as a result of the screened electrostatic repulsion.<sup>37</sup> This is reasonable as for a 10 mM NaCl content the Debye screening length becomes  $33\text{ \AA}$ , i.e., already smaller than the average distance between the structural units.

For the two samples with very low concentrations of electrolyte, i.e., 3 and 4 mM NaCl, it is interesting to note that the correlation peak observed at  $0.06\text{ \AA}^{-1}$  is more pronounced than for the case without added salt. Evidently, the repulsive interaction becomes more pronounced upon the addition of small amounts of electrolyte. The relative decrease in intensity at low- $q$  compared to the most screened sample can be understood as an ordering due to the electrostatic repulsion, which is stronger for the low-salt samples than for the sample with a minimum of ionic strength. At first glance, the observation of more repulsive interactions in a system with small amounts of electrolyte compared to the no-salt system is difficult to comprehend. However, a known salt effect is the enhancement of self-aggregation, reflected as a lowering of the surfactant CMC.<sup>42</sup> Thus, it is possible that small amounts of added electrolyte increase the number of associated surfactant monomers and increase the surface charge and consequently the repulsive interaction between complexes. With larger amounts of electrolyte the screening effect dominates with attractive interactions as a result.

**5. Structuring over Time.** Three samples, prepared to develop into  $L_1$ , G, and a two-phase dispersion of the same ( $G + L_1$ ) were measured three times: 1 day, 2–3 days, and 4 weeks after preparation. The gel sample was in addition measured again after 4 and 7 months. The intention was to gain information on how the gel phase is formed, and the results are presented in Figure 7.

All three samples can be described by the same two features. First, a correlation peak at  $0.07\text{ \AA}^{-1}$  that becomes less intense with time and, for the two samples with gel aggregates, is even originally only little pronounced and then almost disappears. Second, an increase in the lower  $q$  range is observed that levels off after 4 months of equilibration time.

The sample prepared within the  $L_1$  phase shows the first days only scattering from the repulsive interaction between discrete objects. We interpret this as the existence of protein–surfactant micelles in fresh solutions with high surfactant-to-protein ratios.

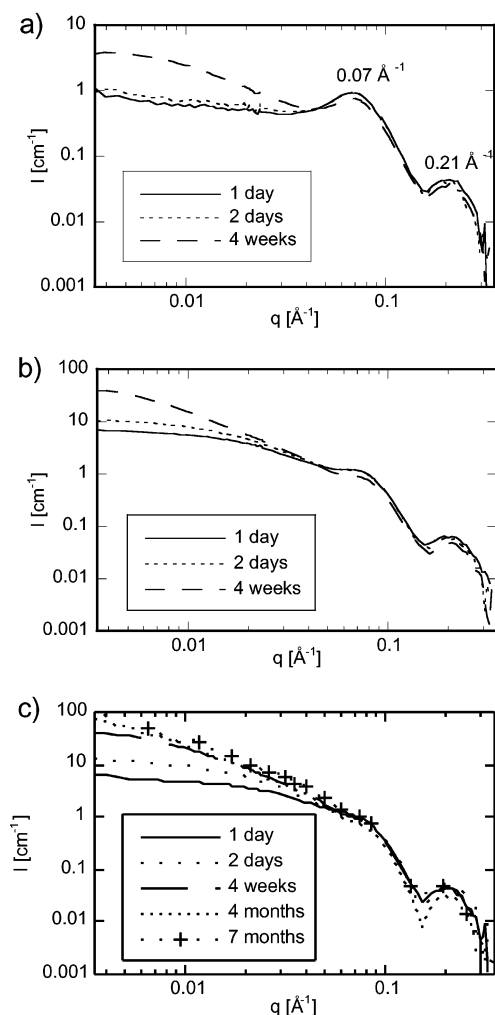


**Figure 7.** Scattering of three different samples measured subsequent times. Contrast IV, i.e., mainly the lysozyme, will contribute to the contrast. (a) Sample prepared in the  $L_1$  region. (b) Sample prepared in the two-phase region of gel and  $L_1$ . (c) Sample prepared in the gel region.

With time the intensity of the correlation peak decreases and the scattering in the lower  $q$  range increases, indicating an aggregation process or a more attractive interaction profile. The authors contend that this is an important issue to explore further as the system expresses phases with long equilibration times.

The two samples with more or less gel character seen in Figure 7b,c, i.e., bluish solutions and gel, evolve in fashions very similar to each other. Both are already, after 1 day, showing a large increase in the lower  $q$  range, which indicates an ongoing aggregation process. The intensity at low  $q$  levels off for the first measurements, indicating a finite size of the dispersed gel aggregates. The intensity at low  $q$  is increasing with time in an almost identical way for the two samples. This is expected as the macroscopic apprehension of the gel before gelation is exactly the same as of the bluish dispersion. The evolving gel can after 4 weeks be superimposed to the ones equilibrated in salt solution (Figure 6b). The correlation at ca.  $0.07 \text{ \AA}^{-1}$  could in the beginning be described as a peak but, with time, the shape is better described as a kink, and it is possible to conclude that the correlation is gone all together after an additional month of equilibrating. This is consistent with the peak being absent in the case of the samples prepared well in advance of the SANS experiments. We regard the disappearance of the correlation as the decrease in the number of discrete protein–surfactant micelles and/or, in the case of the blue solution, as a decrease

in the number of free surfactant micelles. The characteristic size of the system, i.e., the building blocks of the gel, is increasing with time. The continued evolution can in the case of the viscous gel-containing samples be explained by the known long equilibrium times.

When all scattering curves are normalized to the first one measured for the  $L_1$  solution, the relative differences for the evolving structures are seen more clearly. One gel sample from the “salt series” was also measured two times with 1 month in between. Following the same analytical procedure as explained above (normalizing the intensity to the most screened gel in the same contrast), it is clear that the gel becomes more ordered over time, also still changing more than 1 month after preparation. We add this to other indications reported earlier on the gel as a thermodynamically stable phase with a structure that is only slowly reached due to the delicate balance between the hydrophobic attraction and the electrostatic repulsion. To form larger aggregates, relatively large particles have to diffuse and their concentration is low. Furthermore, an aggregation process will be slowed by electrostatic long-range repulsion.

## Conclusions

A contrast variation SANS experiment has been applied to a protein–surfactant system, lysozyme–SDS–water. Two different protein–surfactant aggregates in water have been studied, the soluble complex and the gel. In both aggregates, the protein seems to have retained its globular shape. We conclude that this is in line with results from NMR diffusion<sup>24</sup> and also from Raman spectroscopy. From the latter it is observed that S–S bridges are present still in the two aggregates; however, the peak from the vibrations at  $508 \text{ cm}^{-1}$  is less pronounced for the aggregates compared to pure aqueous protein solutions. Thus our results are different from the ones obtained for more flexible proteins that form necklace-model structures with an unfolded protein polymer associated to surfactant micelles. For the soluble complexes, there is nonetheless an increase at low  $q$  values that indicates an aggregation of proteins. We interpret this to be due to a weak attractive potential (caused by dipolar and/or hydrophobic interactions) that is the basis for a nonpermanent, weakly bound fractal structure. Such transient clustering has recently been reported for other globular proteins.<sup>43,44</sup> The high surfactant-to-protein ratio leads to an opposing, repulsive force that confers the dynamic character of the structure.

The proposed gel structure is similar to that of the micellar solution. However, in the gel phase the lysozyme molecules are much more strongly bound and form much more rigid and permanent one-dimensional aggregates. The stiffness of this aggregation is reflected in the macroscopic elastic properties of the gel.<sup>36</sup>

The continued time evolution of the scattering curves in the case of the viscous gel-containing samples can be explained by the known long equilibrium times. This structure needs weeks to evolve because any protein–surfactant aggregate soluble in solution must be charged and the repulsive interactions are of a longer range than the hydrophobic attraction responsible for the eventual aggregation. It is interesting to note that even for the  $L_1$  sample, which retains the low viscosity and isotropic character throughout the study, a similar time effect of the structural evolution is observed.

Finally, the salt study reproduces the expectation that addition of electrolyte screens the electrostatic repulsion that prevents the gel structure from collapse. However, due to the use of the complex salt,  $\text{Ly}(\text{DS})_8$ , it has been possible to study the system in the absence of even the naturally occurring buffer salts. This



showed that the ionic strength needed to affect the gel structure is lower than the one caused by the salts used at the crystallization of lysozyme. However, a small amount of salt has the opposite effect on the system; i.e., it renders the system an even more repulsive character.

**Acknowledgment.** A.S. was funded by Stiftelsen Strategisk Forskning-Colloidal and Interface Technology. G.M. is grateful to the Ministerio de Educación y Cultura of Spain of Spain for financial support. The Institute Laue-Langevin, Grenoble, France, is thanked for financial support of the SANS experiments. Finally, A.S. thanks Ulf Olsson for valuable discussions and Ali Khan and Håkan Wennerström for the initiative to use SANS.

**Supporting Information Available:** Detailed composition of the samples. This material is available free of charge via the Internet at <http://pubs.acs.org>.

## References and Notes

- (1) Smith, L. J.; Sutcliffe, M. J.; Redfield, C.; Dobson, C. M. *J. Mol. Biol.* **1993**, 229, 930.
- (2) Blake, C. C. F.; Koenig, D. F.; Mair, G. A.; North, A. C. T.; Phillips, D. C.; Sarma, V. R. *Nature* **1965**, 206, 757.
- (3) Creighton, T. E. *Proteins: Structures and Molecular Properties*, 1st ed.; W. H. Freeman and Company: New York, 1983.
- (4) Tanford, C.; Wagner, M. L. *J. Am. Chem. Soc.* **1954**, 76, 3331.
- (5) Price, W. S.; Tsuchiya, F.; Arata, Y. *J. Am. Chem. Soc.* **1999**, 121, 11503.
- (6) Imoto, T.; Johnsson, L. N.; North, A. C. T.; Phillips, D. C.; Rupley, J. A. Vertebrate lysozymes. In *The enzymes*, 3rd ed.; Boyer, P. D., Ed.; Academic Press: New York, 1975, 1736.
- (7) Jones, M. N.; Manley, P. *J. Chem. Soc., Faraday Trans. 1* **1979**, 75, 1736.
- (8) Jones, M. N.; Manley, P. *J. Chem. Soc., Faraday Trans. 1* **1980**, 76, 654.
- (9) Morén, A. K.; Khan, A. *Langmuir* **1995**, 11, 3636.
- (10) Stenstam, A.; Khan, A.; Wennerström, H. *Langmuir* **2001**, 17, 7513.
- (11) Mathis, A.; Zana, R. *Colloid Polym. Sci.* **2002**, 280, 968.
- (12) Jones, M. N.; Manley, P. Thermodynamic studies on the interaction between lysozyme and sodium n-dodecyl sulphate in aqueous solutions. In *Surfactants in Solution*, 4th ed.; Mittal, K. L., Lindman, B., Eds.; Plenum: New York, 1984.
- (13) Guo, X. H.; Zhao, N. M.; Chen, S. H.; Teixeira, J. *Biopolymers* **1990**, 29, 335.
- (14) Ibel, K.; May, R. P.; Kirschner, K.; Szadkowski, H.; Mascher, E.; Lundahl, P. *Eur. J. Biochem.* **1990**, 190, 311.
- (15) Valstar, A.; Brown, W.; Almgren, M. *Langmuir* **1999**, 15, 2366.
- (16) Reynolds, J. A.; Tanford, C. *J. Biol. Chem.* **1970**, 245, 5161.
- (17) Shirahama, J. *Biochemistry* **1974**, 75, 309.
- (18) Lundahl, P.; Greijer, E.; Sandberg, M.; Cardell, S.; Eriksson, K.-O. *Biochim. Biophys. Acta* **1986**, 873, 20.
- (19) Nicoli, D. F.; Benedek, G. B. *Biopolymers* **1976**, 15, 2421.
- (20) Muschol, M.; Rosenberger, F. *J. Chem. Phys.* **1995**, 103, 10424.
- (21) Tani, F.; Murata, M.; Higasa, T.; Goto, M.; Kitabatake, N.; Doi, E. *Biosci. Biotech. Biochem.* **1993**.
- (22) Doi, E. *Trends Food Sci. Technol.* **1993**, 4, 1.
- (23) Clark, A. H.; Judge, F. J.; Richards, J. B.; Stubbs, J. M.; Suggett, A. *Int. J. Peptide Protein Res.* **1981**, 17, 380.
- (24) Stenstam, A.; Topgaard, D.; Wennerström, H. *J. Phys. Chem. B* **2003**, 107, 7987.
- (25) Gripon, C.; Legrand, L.; Rosenman, I.; Vidal, O.; Robert, M. C.; Boué, F. *J. Cryst. Growth* **1997**, 178, 575.
- (26) Ghosh, R. E.; Egelhaaf, S. U.; Rennie, A. R. *A Computing Guide for Small-Angle Scattering Experiments*; Institute Max von Laue Paul Langevin, 2000.
- (27) Chen, S. H.; Teixeira, J. *Phys. Rev. Lett.* **1986**, 57, 2583.
- (28) Teixeira, J. *J. Appl. Crystallogr.* **1988**, 21.
- (29) Velev, O. D.; Kaler, E. W.; Lenhoff, A. M. *Biophys. J.* **1998**, 75, 2682.
- (30) Cabane, B. In *Surfactant Solutions – new methods of investigation*; Zana, R., Ed.; Marcel Dekker: New York, 1987; p 57.
- (31) Baba-Ahmed, L.; Benmouna, M.; Grimson, M. *J. Phys. Chem. Liq.* **1987**, 16, 235.
- (32) Hamaguchi; Sakai, J. *Biochemistry* **1965**, 57, 721.
- (33) Sochava, I. V.; Belopolskaya, T. V. *Food Hydrocolloids* **1992**, 6, 97.
- (34) Jones, J. A.; Wilkins, D. K.; Smith, L. J.; Dobson, C. M. *J. Biomol. NMR* **1997**, 10, 199.
- (35) Morén, A. K.; Regev, O.; Khan, A. *J. Colloid Interface Sci.* **1999**, 222, 170.
- (36) Montalvo, G.; Khan, A. Submitted to *Langmuir*.
- (37) Renard, D.; Axelos, M. A. V.; Boué, F.; Lefebvre, J. *Biopolymers* **1996**, 39, 149.
- (38) Quina, F. H.; Nassar, P. M.; Bonilha, J. B. S.; Bales, B. L. *J. Phys. Chem.* **1995**, 99, 17028.
- (39) Cabane, B.; Duplessix, R. *J. Physique* **1982**, 43, 1529.
- (40) Morén, A. K.; Nydén, M.; Söderman, O.; Khan, A. *Langmuir* **1999**, 15, 5480.
- (41) Porte, G.; Marignan, J.; Basseau, P.; May, R. P. *Europhys. Lett.* **1988**, 7, 713.
- (42) Gunnarsson, G.; Jönsson, B.; Wennerström, H. *J. Phys. Chem.* **1980**, 84, 3114.
- (43) Piazza, R.; Iacopini, S. *Eur. Phys. J. E* **2002**, 7, 45.
- (44) Oates, K. M. N.; Krause, W. E.; Jones, R. L.; Colby, R. H. Manuscript in preparation.